



Article

Improvement of CO₂ Photoreduction Efficiency by Process Intensification

Zekai Zhang ^{1,*}, Ying Wang ¹, Guokai Cui ¹ , Huayan Liu ¹, Stéphane Abanades ²  and Hanfeng Lu ^{1,*}

¹ Institute of Chemical Reaction Engineering, College of Chemical Engineering, Zhejiang University of Technology, Chaowang Road 18, Hangzhou 310014, China; wang17757192353@163.com (Y.W.); chemcgk@163.com (G.C.); hylu@zjut.edu.cn (H.L.)

² Processes, Materials and Solar Energy Laboratory, PROMES-CNRS (UPR 8521), 7 Rue du Four Solaire, 66120 Font-Romeu, France; stephane.abanades@promes.cnrs.fr

* Correspondence: zzk@zjut.edu.cn (Z.Z.); luhf@zjut.edu.cn (H.L.)

Abstract: This paper addresses an innovative approach to improve CO₂ photoreduction via process intensification. The principle of CO₂ photoreduction using process intensification is presented and reviewed. Process intensification via concentrating solar light technology is developed and demonstrated. The concept consists in rising the incident light intensity as well as the reaction temperature and pressure during CO₂ photoreduction using concentrating solar light. A solar reactor system using concentrated sunlight was accordingly designed and set up. The distribution of light intensity and temperature in the reactor was modeled and simulated. CO₂ photoreduction performance in the reactor system was assessed, and the reaction temperature and pressure evolution were recorded. The results showed that the light intensity, temperature, and pressure could be effectively increased and irradiation on the catalyst surface followed a Gaussian distribution. The CO₂ photoreduction reaction rates were enhanced to hundreds of times.

Keywords: CO₂ photoreduction; process intensification; concentrated solar light; reaction kinetics



Citation: Zhang, Z.; Wang, Y.; Cui, G.; Liu, H.; Abanades, S.; Lu, H. Improvement of CO₂ Photoreduction Efficiency by Process Intensification. *Catalysts* **2021**, *11*, 912. <https://doi.org/10.3390/catal11080912>

Academic Editor:
Consuelo Alvarez-Galvan

Received: 17 June 2021
Accepted: 26 July 2021
Published: 28 July 2021

Publisher's Note: MDPI stays neutral with regard to jurisdictional claims in published maps and institutional affiliations.



Copyright: © 2021 by the authors. Licensee MDPI, Basel, Switzerland. This article is an open access article distributed under the terms and conditions of the Creative Commons Attribution (CC BY) license (<https://creativecommons.org/licenses/by/4.0/>).

1. Introduction

CO₂ and other greenhouse gas emissions from carbon-based energy resources have caused many environmental and societal problems. CO₂ capture and utilization is a profitable route to limit CO₂ content in the air and reach carbon neutral energy production [1]. Among the different ways of CO₂ utilization, CO₂ photoreduction, which can reduce CO₂ molecules into valuable fuels and chemicals via solar energy, is thought to be a fundamental pathway to decrease CO₂ emission, store solar energy, and realize the carbon cycle, as described in Equation (1).



The global CO₂ photoreduction process is similar to the effect of photosynthesis performed by plants; therefore, it is also called artificial photosynthesis. In the 1970s, Fujishima and Honda [2,3] first carried out the study of this topic. Since then, the subject has been extensively studied and the works have been summarized in many extensive reviews [4–26]. Significant process progress has been made, especially regarding the development of novel catalytic systems. However, CO₂ photoreduction is a complex technology and additional research works are still needed before the process can be used in practical applications.

A major issue is the solar-to-chemical (STC) energy conversion efficiency of the CO₂ photoreduction process. Solar energy is a low-density energy resource. With limited radiation, a high STC efficiency is fundamental to obtain substantial products from CO₂ in the specific area of the “solar farm”. Unfortunately, the reported STC efficiency from the

different sources is not comparable with photovoltaic or photothermal power generation paths at present. Only a few reported values exceed the photosynthetic efficiency of green plants (0.4%). The main challenges in CO₂ photoreduction are to effectively improve the STC efficiency, increase the reduction rate of CO₂, and obtain high value hydrocarbon products with multiple carbon atoms.

The current reasons accounting for the low STC efficiency of the process lie in many aspects. First, the bond energy of C=O is about 750 kJ/mol, which makes CO₂ an extremely stable compound and hard to be activated. Secondly, the reduction of CO₂ to hydrocarbons involves different steps, including a series of fracture and formation of different bonds between carbon, oxygen, and hydrogen atoms, and the overall mechanism is very complex. A competition behavior also happens between the CO₂ photoreduction and H₂O splitting. The latter is relatively easy, as H₂O is directly decomposed into H₂ instead of forming H⁺ to continue to participate in the reaction with CO₂ [27,28].

As the properties of CO₂ molecules are not favorable, the possible approaches to improve the CO₂ photoreduction efficiency are related to the photocatalysts and reaction conditions. However, it is still difficult to tackle the problem only through developing new catalysts at present. The main reason is the easy recombination of photogenerated e⁻-h⁺ pairs.

In addition to the photocatalyst, the reaction environment and operating conditions of CO₂ photoreduction should be paid more attention. At present, research on CO₂ photoreduction is mainly carried out in a reaction environment close to mild natural conditions, i.e., the reaction conditions are imposed and require to find a flexible catalyst. Alternatively, a different reaction environment can be proposed along with other suitable catalysts developed for the new reaction environment. Accordingly, the CO₂ photoreduction may be realized via process intensification.

The mild reaction conditions may be part of the reasons for the low STC efficiency of CO₂ photoreduction. First, it induces a mismatch of reactant concentration. For the reaction in liquid phase at room temperature (25 °C), the CO₂ solubility in water is limited to about 33 mmol/L. Meanwhile, if the reaction is in the gas phase, the saturated H₂O vapor pressure would be limited to 3.2 kPa. Obviously, whether the reaction is carried out in gas or liquid phase, the concentration of one reactant is always limited, which affects the CO₂ reduction reaction rate. In addition, the low flux density of solar energy limits the amount of reaction products per unit area. The distribution of reactants in the reactor and the collection of products are also hard to operate. If the industrial CO₂ photoreduction is still operated under such mild temperature and pressure conditions, the scale of the reactor and catalyst will need to be as large as the size of a solar farm. The associated cost of the catalyst and reactor will thus be rather considerable. A more practical reaction environment and operating conditions should thus be considered.

Some studies have showed that the CO₂ photoreduction can be improved by the reaction conditions intensification. Although the photocatalytic reduction of CO₂ is a photo-induced reaction, it cannot remove the influence of thermodynamics. In other words, the CO₂ photoreduction process is not simply a light-driven reaction, but also a photo-thermal reaction. Increasing the light intensity, reaction temperature, and pressure may not only facilitate the reaction shift to the products side, but also should have a substantial effect on the performance of CO₂ photoreduction, just as Prof. Grimes says, "We believe gas phase photoreduction of CO₂ and water vapor under concentrated sunlight is the most promising pathway to develop a viable CO₂ to fuel conversion technology" [9], which hints at a new reaction environment with high light intensity and high reaction temperature conditions.

The temperature increase also brings the concept of "photothermal chemistry" or "photothermal catalysis" [21]. In this viewpoint, CO₂ photoreduction process is an integration of the photochemical and the thermochemical processes. Gascon et al. [25] proposed a review of photothermal catalysis. In contrast to thermochemical processes (using heat input to the whole reaction environment), the photothermal route is mainly originated from

the localized surface plasmon resonance effect, which can be realized by the interaction between the regular light source and the catalyst with certain elements and structure to create a high temperature on the local surface of the catalyst. Thermochemistry mainly relates to the influence of the reaction conditions, while photochemistry mainly addresses the development of new catalyst systems. Luque and Colmenares [28] used a new term “Thermo-Photocatalysis” and broadened the topic to other photocatalysis reactions such as volatile organic compounds (VOCs) degradation.

In this work, beyond the influence of temperature, other parameters such as light intensity and pressure are also investigated. The concept of “process intensification” is thus introduced to describe the situation. Process intensification represents one of the most active fields for modern chemical engineering [29]. It considers all the means to improve the efficiency of the transport processes ranging from charge carrier transfer in the catalyst nanoparticles to reactant transfer in the reactor. In this work, special focus is brought to the influence of operating parameters on the CO₂ photoreduction reaction.

2. Progress of Process Intensification in CO₂ Photoreduction Process

2.1. Reaction Kinetic Model of CO₂ Photoreduction

The process intensification addresses the transport phenomena during the CO₂ photoreduction, which includes but is not restricted to parameters such as the solar light intensity, T and P. These parameters can be directly reflected in the reaction kinetics of CO₂ photoreduction. However, few reports have dealt with this issue. Tan et al. [30] derived a reaction rate equation via the Langmuir-Hinshelwood (L-H) mechanism (Equation (2)).

$$\text{Rate} = (kI^\alpha K_{\text{H}_2\text{O}} K_{\text{CO}_2}) \left(\frac{P_{\text{H}_2\text{O}} P_{\text{CO}_2}}{(1 + K_{\text{H}_2\text{O}} P_{\text{H}_2\text{O}} + K_{\text{CO}_2} P_{\text{CO}_2})^2} \right) \quad (2)$$

It is a typical rate law equation formula for the heterogeneous catalytic reaction, except the item I^α , which represents the reaction order of the light intensity. The authors then systematically varied the operation parameters and determined the most suitable reaction conditions. Based on the collected data of the reaction rate, the light intensity and pressure, the kinetic parameters were obtained via the regression method. The maximum reaction rate was determined to be 84.42 $\mu\text{mol}\cdot\text{g}^{-1}\cdot\text{h}^{-1}$. The two adsorption equilibrium constants, K_{CO_2} and $K_{\text{H}_2\text{O}}$, were also determined. The values of K_{CO_2} (0.019 bar^{-1}) and of $K_{\text{H}_2\text{O}}$ (8.07 bar^{-1}) implied that the adsorption of H₂O was much stronger than CO₂ on the catalyst surface.

Olivo et al. [31] investigated the effect of reaction time and irradiance on the CO₂ photoreduction in two different reactors. At low light intensity, the catalyst surface is not saturated with incident photons, therefore, reaction time prolonging and light intensity increment will be significantly helpful to the CO₂ photoreduction. Using a low intensity light source (40–60 W m^{-2}), both temperature and reaction time significantly affected CO₂ photoreduction. The maximum yield of CH₄ production reached about 28.50 $\mu\text{mol}\cdot\text{g}^{-1}$ (for 40 W m^{-2}) after 4 h. Under this situation, it is the photoexcitation that restricts the overall STC efficiency. Meanwhile, at high light intensity, the catalyst surface seems to be saturated by photons and the light increment does not affect photocatalytic reduction any more, while the time prolonging is still important to the CO₂ conversion. When using a high intensity light source (60–2400 W m^{-2}), the maximum CH₄ production of 0.19 $\mu\text{mol}\cdot\text{g}^{-1}$ was obtained (for 1240 W m^{-2}) after 2 h.

Olivo et al. [32] then studied the influence of molar ratio of CO₂/H₂O reactants on the CO₂ photoreduction. With the decrease of the CO₂/H₂O molar ratio, the CH₄ yield showed a bell-shaped trend. They considered that it was the result of the competition reaction between CO₂ photoreduction and water splitting and the competition between the CO₂ and H₂O adsorption. That is to say, the CO₂ photoreduction is a two-reactant reaction, and the adsorption of both reactants is important. When the CO₂/H₂O molar ratio is much lower and CO₂ adsorption is too weak, the excess absorbed H₂O would be split into H₂ and

O₂. These works disclosed the effect of reaction parameters on the catalytic performance of CO₂ photoreduction, but they did not formulate the reaction rate law.

Khalilzadeh [33] investigated the influence of CO₂ and H₂O partial pressure on the activity of iron and nitrogen-modified TiO₂ photocatalysts for CO₂ photoreduction and formulated a kinetic model based on the L-H mechanism (Equation (3)).

$$\text{Rate} = kI^\alpha \left(\frac{(b_{\text{CO}_2}P_{\text{CO}_2})^{1/n} (b_{\text{H}_2\text{O}}P_{\text{H}_2\text{O}})^{1/n}}{(1 + (b_{\text{CO}_2}P_{\text{CO}_2})^{1/n} + (b_{\text{H}_2\text{O}}P_{\text{H}_2\text{O}})^{1/n})^2} \right) \quad (3)$$

The related rate constants were obtained via experimental data regression; α value is 0.65, b_{CO_2} value is 22.74 bar⁻¹, $b_{\text{H}_2\text{O}}$ value is 145.2 bar⁻¹, n value is 1.23 and k value is 6.47 $\mu\text{mol}\cdot\text{g}_{\text{cat}}^{-1}\cdot\text{h}^{-1}$. The maximum yield rate of CH₄ is 28.15 $\mu\text{mol}\cdot\text{g}^{-1}\cdot\text{h}^{-1}$.

Delavari [34] used three different Hg lamps (50 W, 150 W, and 250 W) as UV light sources and studied the CH₄ dry reforming reaction with CO₂ on the TiO₂. UV light with the largest power (250 W) was found to give the highest STC efficiency under the tested reaction conditions. They also developed a reaction kinetic model using the Langmuir–Hinshelwood mechanism (Equation (4)).

$$\text{Rate} = (k_1 I^\alpha K_{\text{CH}_4} P_{\text{CH}_4} K_{\text{CO}_2} P_{\text{CO}_2}) / N \quad (4)$$

$$N = (1 + K_{\text{CH}_4} P_{\text{CH}_4} + K_{\text{CO}_2} P_{\text{CO}_2} + K_{\text{C}_2\text{H}_6} P_{\text{C}_2\text{H}_6} + K_{\text{CH}_3\text{COOH}} P_{\text{CH}_3\text{COOH}} + \text{etc})^2$$

The results showed that the reaction rate of CH₄ dry reforming is proportional to P_{CO_2} at a very low partial pressure. The reason is considered to be that only a small fraction of the active sites are occupied, similar to [32]. Meanwhile, as CO₂ partial pressure increases, the linear relation would be broken, possibly due to the full coverage of CO₂ on the catalyst surface. The best fitted reaction kinetic constants are listed as follows: α value is 0.75, K_{CO_2} value is 15 bar⁻¹, $K_{\text{H}_2\text{O}}$ value is 50 bar⁻¹, I value is 150 mW cm⁻² and k value is 117 $\mu\text{mol} - \text{g}_{\text{cat}}^{-1}$ [35].

2.2. Influence of Reaction Temperature on CO₂ Photoreduction Performance

For the effect of temperature, we do not emphasize the photothermal catalysis with the localized surface plasmon resonance effect, but rather focus on the studies that aimed to improve the reaction rate through increasing the reaction temperature of the system. These studies are relatively scarce.

Singhal et al. [36] evaluated the CO₂ photoreduction in the gas phase with a noble metal-modified TiO₂ and were especially concerned with the temperature effect. CH₄ and C₂H₆ were observed as the products. They found that the maximum reaction rate was reached at 25 °C, and 1.787 $\mu\text{mol}\cdot\text{g}^{-1}\cdot\text{h}^{-1}$ of CH₄ and 0.212 $\mu\text{mol}\cdot\text{g}^{-1}\cdot\text{h}^{-1}$ of C₂H₆ were produced. A higher or lower temperature would cause a decrement of the reaction rate.

The concern with the Debye temperature of semiconductor materials is one of the main reasons for the few studies on high temperature photocatalysis, which will accelerate the recombination of e⁻-h⁺ pairs. Poudyal et al. [37] stated that the combination of thermal and photon energy inputs may be possible and that some higher temperatures would not influence the recombination rate too much. Developing some semiconductors with a high Debye temperature is also a reasonable method, where recombination does not outstrip reaction rates. They studied CO₂ photoreduction in the gas phase on the four semiconductors SiC, Si, Pt/TiO₂, and GaN at two high temperatures (250 °C and 350 °C). The results revealed that the semiconductors that possess high Debye temperatures facilitate C–O cleavage and CO₂ photoreduction to CH₄. Both C–O cleavage and H₂O dissociation steps can be thermally promoted at high temperatures, which increases CH₄, CO, and H₂ yield.

Bao et al. [38] investigated CO₂ photoreduction with H₂O using Co nano-microstructured catalysts and obtained different long-chain alkanes. Different from the plasmonic effect, they believed that the production of the long chain alkanes is promoted by the photo-

thermal energy. The heating temperature of the Co catalysts is found to be about 160 °C, i.e., the reaction happens at this temperature.

Ma's group [39] realized selectivity tuning of CO₂ photoreduction over Fe-based catalysts and thought the process is a photothermal process via light irradiation. A full CO selectivity (about 100%) was obtained on the used Fe₃O₄ catalyst. A reaction rate of 11.3 mmol·g⁻¹·h⁻¹ at 350 °C indicated the process is a photothermal catalytic conversion of CO₂. More interestingly, they got a pure θ-Fe₃C phase, which provided high product selectivity to hydrocarbons (>97%) and a superior reaction rate (10.9 mmol·g⁻¹·h⁻¹) at 350 °C via the photothermal effect.

Ozin et al. [40] recorded the temperature dependence of the thermal and photothermal CO₂ reduction, i.e., the CO₂ reduction driven by photothermal and thermal effect only. A clear light effect appeared at 120 °C and increased continually to 300 °C, which enhanced reaction rates and decreased the observed activation energy. Corresponding Arrhenius plots exhibited a highly linear behavior, resulting in a thermal activation energy of 89 kJ mol⁻¹ and a photothermal activation energy of 64 kJ mol⁻¹ for the reverse water-gas shift (RWGS) reaction under dark and light conditions, respectively.

Bai et al. [41] employed Bi/Bi₄O₅I₂ composites as catalyst. Under a simulated sunlight source, the CO and CH₄ generation rate over Bi/Bi₄O₅I₂ was increased to 40.02 and 7.19 mmol·g⁻¹·h⁻¹, respectively. The STC efficiency was about 68.55 times higher in comparison with Bi₄O₅I₂ without the temperature rising. The dramatically enhanced activity of Bi/Bi₄O₅I₂ was thereby attributed to the photothermal effects.

Zhang et al. [42] put forward the idea of direct coupling the thermo and photo-effects to enhance the CO₂-H₂O reaction with a bifunctional Au-Ru/TiO₂ catalyst. A 15 times higher activity was obtained in comparison with the water splitting. At 85 °C, around 99% CH₄ selectivity was reached. During the single thermos-catalytic reaction, 356 mmol·g⁻¹·h⁻¹ of CH₄ was produced at 85 °C. At the same temperature, a combination of thermo-photocatalytic effects was observed.

It is known that CO₂ methanation cannot happen under ambient sunlight. Ye et al. [43] thereby constructed a photothermal reactor system using a selective light absorber and generated a very high temperature with natural incident solar light (1 kW·m⁻²). The system offered a temperature up to 288 °C, which is three times higher than that in the traditional systems. As a result, CO₂ conversion of 80% and CH₄ yield rate of 7.5 L·m⁻²·h⁻¹ were obtained on a Ni/Y₂O₃ catalyst with real solar irradiation.

Li et al. [44] investigated the photo-thermocatalytic performance of syngas to olefins with a Mn-based catalyst. The reaction temperature was selected to be 250 °C. A good selectivity of 27.0% for light olefins and a ratio of olefins to paraffins equal to 3:2 were obtained. Although the work is more related to the catalytic material, the photothermal effect and the temperature influence is clear.

2.3. Intensification of Light Intensity to Improve the CO₂ Photoreduction Performance

Regarding a light-driven reaction, the incident light intensity is a key parameter that affects the reaction activity. However, there are very few studies concerning the light intensity influence, because light intensity is not a simple parameter to investigate. Light wavelength also needs to be considered. To favor photocatalysis, the incident light should provide a photon energy threshold. The light with a shorter wavelength and high energy is significantly more effective than that the light with a longer wavelength and low energy [45]. As most of the studies use an artificial light source, a suitable light wavelength can be guaranteed while the light intensity is, conversely, hard to be adjusted and studied. Nonetheless, recalling [35], the UV light power of 250 W with the highest light intensity offered the highest reaction rate under the experimental conditions, indicating the effect of light intensity. Some reports other than CO₂ photoreduction may give some hints on the H₂ evolution reduction and NO reduction [46,47].

2.4. Intensification of the Reactant Pressure

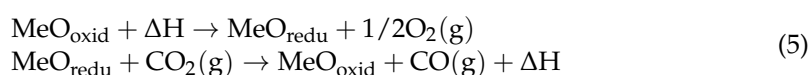
Reactant pressure is relative to the concentration of a reactant. Rossetti et al. [44] noticed that CO₂ solubility is severely limited in liquid water. The relatively high temperature, which favors the reaction kinetics, definitely caused a very poor productivity in the liquid phase. To overcome this problem, they put forward a new type of photoreactor, which can operate under very high pressure (up to 20 bar). A high pressure is expected to improve the CO₂ solubility in water even at a high reaction temperature.

The effect of high reactor pressure for CO₂ photoreduction was tested using a standard photocatalyst (Degussa P25) and resulted in 120 mmol kg⁻¹ of CH₄ at the conditions of 10 bar and room temperature (25 °C) after 6 h of reaction. When the reaction pressure and temperature were increased to 20 bar and 85 °C, a gaseous products mixture with H₂, CH₄, and other C1–C2 products was yielded in the liquid phase. The obtained values of H₂ and CH₄ were as high as 51.2 mmol h⁻¹ kg_{cat}⁻¹ and 1.73 mmol h⁻¹ kg_{cat}⁻¹, respectively. The results suggest a complex process consisting of CO₂ photoreduction and photo reforming of products in the reactor. In general, the concept of the high pressure reactor was proved. The high pressure improved the product yield and allowed the high reaction temperature, which led to the higher productivity and disclosed a direct dependence of products distribution on pressure and temperature. The productivity was significantly higher than the representative results reported in the literature [48,49].

More tests brought the conclusion that high pressure favors the accumulation of CO₂ photoreduction products in liquid phase, whereas an intermediate pressure is beneficial to increase the productivity of the gas phase species.

2.5. High Flux Irradiation by Concentrated Solar Light

Concentrating light technology can provide high-flux solar radiation (multiple suns intensity) and raise both the incident light intensity and temperature, which is an interesting way to yield an intensification effect of diverse reaction conditions. However, concentrating solar power is more developed in the two-step thermochemical CO₂-splitting route for operating the high-temperature reactions toward CO (and/or H₂) and regenerating the redox catalyst with the following steps (Equation (5)).



Few studies attempted to transfer the technology to the CO₂ photoreduction process. Singh et al. [36] used concentrated sunlight as the light source and developed a model to explain the photo-physics pattern that controlled the photogeneration, recombination, charge trapping, and multielectron photocatalytic reduction of adsorbed species on TiO₂ nanoparticles. A linear relationship between the photocatalytic reaction rate and the photogeneration rate is expected, and the observed results responded to this expectation. That is to say, the multielectron photocatalytic reduction rate can be enhanced by concentrating sunlight intensity.

Guan et al. [50,51] first constructed an experimental set-up and then investigated two catalytic systems under concentrated sunlight; one is a combination of Pt-loaded K₂Ti₆O₁₃ with Cu/ZnO and another is Pt-loaded K₂Ti₆O₁₃ photocatalyst and Fe-based F–T catalyst supported on a dealuminized Y-type (DAY) zeolite. They found that the maximum temperature of the set-up could reach ca. 600 K in October and 540 K in December. The CO₂ photoreduction, especially on the hybrid catalyst using Fe-Cu-K/DAY and Pt/K₂Ti₆O₁₃, was enhanced to a much greater extent than that observed at room temperature, resulting in the formation of different organic compounds such as CH₄, HCOOH, HCHO, CH₃OH, and C₂H₅OH. The study revealed that a photothermal effect could improve the CO₂ photoreduction activity. Basically, it could be considered that the reaction mainly occurred in the liquid, as the catalyst was immersed in the water.

In another study, Nguyen et al. [52] also investigated CO₂ photoreduction with concentrated natural sunlight. The reactor was a continuous circular Pyrex glass reactor (216 cm³)

with a quartz window for the incident sunlight. The sunlight was concentrated using a solar concentrator (Himawari, Tokyo, Japan) surrounding the reactor. A N_3 dye-modified Cu-Fe/TiO₂ catalyst was chosen as the photocatalyst system. Although they focused more on the N_3 dye effect, which broadened the light adsorption band to the visible light range, the concentrated sunlight definitely worked during the process. The CH₄ production rate reaches 0.617 $\mu\text{mol}\cdot\text{g}^{-1}\cdot\text{h}^{-1}$ under concentrated natural light. Only methane was observed as the product, and the reason was attributed to the too low intensity of concentrated sunlight, which might not provide enough driving force to reduce CO₂ to ethylene. Nonetheless, after concentrating of only ca. 20 mW/cm² natural light, the activity on the N_3 dye-modified CuFe/TiO₂ catalyst was comparable to the result using 225 mW/cm² artificial light source. This report again proved the effect of concentrated light on the CO₂ photoreduction.

The above works stimulated the utilization of concentrating solar light in CO₂ photoreduction, however, the studies are not extensively detailed. For example, none mentioned the concentrating light ratio, which is substantial in the concentrating technology. In 2017, Han et al. [53] built an indoor concentrating solar reactor system with an artificial light source and studied CO₂ photoreduction with H₂O using TiO₂ and Pt/TiO₂ catalyst. The effect of the concentrating ratio was noticed for the first time in CO₂ photoreduction. The concentrating ratio was adjusted by varying the distance between the catalyst and the Fresnel lens. The results showed that the CH₄ production was clearly improved by the concentrating light, and the concentrating ratio had an obvious influence on the activity. The maximum CH₄ product was reached at a 12.9 concentrating ratio, and it was about 7 times higher than that obtained under natural (non-concentrating) light intensity. Interestingly, the effect of the concentrating light was not limited to increasing the light intensity or the temperature; it also had an influence on the properties of the catalyst. Li et al. [54] pretreated the TiO₂ catalyst with the concentrating light before reaction, and they found that the CH₄ production rate not only increased from 0.70 $\mu\text{mol}\cdot\text{g}^{-1}\cdot\text{h}^{-1}$ under natural light to 20.67 $\mu\text{mol}\cdot\text{g}^{-1}\cdot\text{h}^{-1}$ under concentrated light, but also further increased to 28.49 $\mu\text{mol}\cdot\text{g}^{-1}\cdot\text{h}^{-1}$ after pretreating the TiO₂ catalyst in air. The results mean that concentrating light increased CO₂ conversion not only by heightening light intensity, but also by improving the surface properties of the catalyst.

Due to the power limitations of the artificial light source, the reaction temperature cannot be raised efficiently, which restrains the effect of concentrating light technology in CO₂ photoreduction. Fang et al. [55] thereby constructed a large concentrating solar light reactor system with a large Fresnel lens (diameter = 1 m) using real solar light source. The system was able to effectively increase the light intensity and the reaction temperature, as well as the pressure of CO₂ and H₂O in the system. The most typical photocatalyst P25 was first chosen to provide comparable results with other reports. The overall CO₂ conversion reaction rate was boosted to thousands of $\mu\text{mol}\cdot\text{g}^{-1}\cdot\text{h}^{-1}$, and more products were detected such as CH₄, C₂H₄, and C₂H₆. The maximum CH₄, C₂H₄, and C₂H₆ yield rates reached 3157.2 $\mu\text{mol}\cdot\text{g}^{-1}\cdot\text{h}^{-1}$, 511.6 $\mu\text{mol}\cdot\text{g}^{-1}\cdot\text{h}^{-1}$, and 1346.0 $\mu\text{mol}\cdot\text{g}^{-1}\cdot\text{h}^{-1}$, respectively. Meanwhile, the CO₂ conversion increased up to 3.94%, and the overall STC efficiency reached 2.12% (based on the UV part) and 0.15% (based on the full solar light spectrum). Such a promising result demonstrates the potential of concentrating solar light technology in CO₂ photoreduction.

Gao et al. [56] then extended the catalyst system to a Fe₂O₃ film using the same reactor system. The main gas products were CH₄, C₂H₄, and C₂H₆. The maximum production rates of CH₄, C₂H₄, and C₂H₆ could reach 1470.7, 736.2, and 277.2 $\mu\text{mol}/(\text{g}\cdot\text{h})$, respectively, and the CO₂ conversion was about 0.78%. Besides the effect of reaction parameters, a Z-scheme mechanism Fe₂O₃/Fe₃O₄ catalyst was put forward to explain the high activity. However, the effect of concentrating solar light needs to be further analyzed.

Based upon the above discussion, it can be concluded that the enhancement of reaction conditions, including the increase of light intensity, temperature, and pressure, are crucial to improve the CO₂ photoreduction reaction rate. In particular, the light concentration results

in the increase of these parameters simultaneously and thereby offers a sharp improvement of the reaction rate. The typical catalyst, TiO₂ (P25), can reach a reaction rate of only several $\mu\text{mol}\cdot\text{g}^{-1}\cdot\text{h}^{-1}$ under common reaction conditions, while it can be enhanced to thousands of $\mu\text{mol}\cdot\text{g}^{-1}\cdot\text{h}^{-1}$ under concentrated solar light [13,56]. On the other hand, the number of studies about reaction intensification is quite low, and the underlying mechanisms for understanding reaction intensification need to further elucidated. Especially for the concentrating light reaction system, promising results have been obtained due to the simultaneous intensification of all the reaction conditions. Therefore, a concentrating solar light reactor was built, and the influence of reaction parameters on CO₂ photoreduction was modeled and investigated.

3. Concentrating Solar Light Reactor System Design and Modeling

3.1. Operating Principle of the Concentrating Solar Light Reactor System

Figure 1 illustrates the schematic view of the concentrating solar light reactor system. It is mainly composed of a reactor and a Fresnel lens concentrator. The reactor is made of a stainless steel material with 5 cm ID and 100 mL volume. A circular disc-shaped catalyst is fixed with a holder in the reactor. Concentrated sunlight is used as the light source. A PMMA Fresnel lens is placed above the window of the reactor, so that incident solar light can be concentrated by passing through the lens and through the glass window to reach the catalyst. The lens diameter is 1 m and the concentration ratio, i.e., the area ratio of the Fresnel lens to the catalyst ($\frac{\pi R_{\text{lens}}^2}{\pi r_{\text{cata}}^2} = \frac{R_{\text{lens}}^2}{r_{\text{cata}}^2}$), can be adjusted. CO₂ and H₂O are injected via the opening on the side wall of the reactor. Detailed parameters are provided in Table 1 and Figure 1.

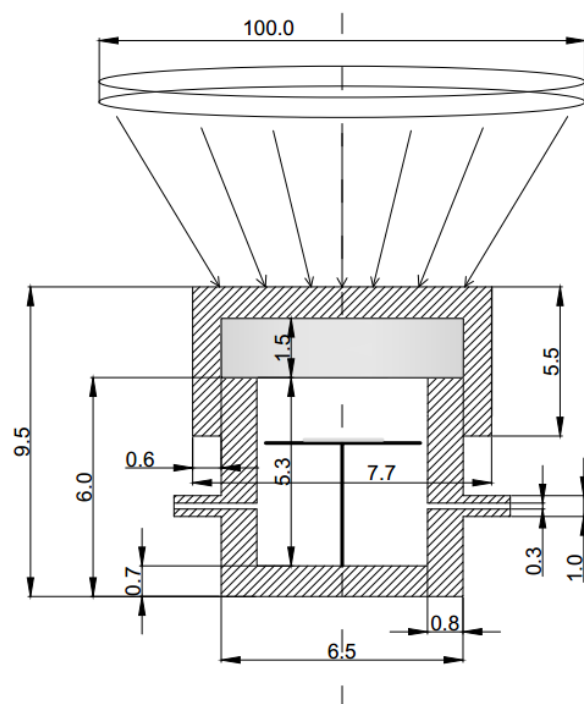


Figure 1. Side view of the concentrating reactor system (unit: cm).

Table 1. Operating parameters of the concentrating solar light reactor system.

System Items	Parameters
Light source	Natural light
Measured light intensity	60 mW/cm ² *
UV band	7%
Fresnel lens diameter	1 m
Reactor ID	5 cm
Reactor OD	6.5 cm
Reactor material	Stainless steel
Reactor volume	100 mL
Catalyst material	TiO ₂
Catalyst shape	Disc
Typical catalyst diameter	1.2 cm
Catalyst weight	40 mg

* Note: natural light is measured at AM 12:00 in Hangzhou.

For such a reactor system, when the sunlight is concentrated, the incident light intensity can be raised to a large extent. Besides the incident light intensity, the energy contained in the sunlight concentrated by the lens (within the area corresponding to the diameter of 1 m) is high enough to heat the reactor, especially the materials (both the reactants and the catalyst), to a very high temperature, which in turn increases the reaction pressure. As mentioned before, the intensification of reaction conditions is expected to influence the reaction performance significantly, both from viewpoints of thermodynamics and kinetics.

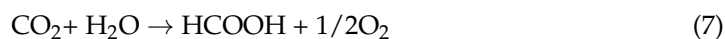
3.2. Reaction Kinetics Analysis

The reaction rate law of CO₂ photoreduction based upon the L-H mechanism has been detailed in Equation (2) [31]. As most CO₂ photoreduction studies are carried out under a constant light intensity at present, the I parameter can be seen as I₀, and kI^α is often simplified to be k'. The reaction rate is then simplified as:

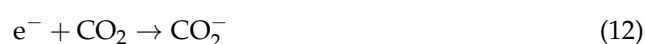
$$-r'_{\text{CO}_2} = k' \frac{P_{\text{H}_2\text{O}} P_{\text{CO}_2}}{(1 + K_{\text{H}_2\text{O}} P_{\text{H}_2\text{O}} + K_{\text{CO}_2} P_{\text{CO}_2})^2} \quad (6)$$

However, when considering the concentrating solar light reactor, the influence of both temperature and light intensity have to be considered and reflected in the equation.

It is admitted that CO₂ photoreduction with H₂O is a very complex heterogeneous photocatalytic process. Many reactions can occur and yield different C1, C2, or even C₃+ hydrocarbons [23].



In fact, these reaction equations are too simple to illustrate the real mechanism of CO₂ photoreduction. As mentioned before, CO₂ photoreduction is a heterogeneous photocatalytic reaction; the process is definitely composed of a series of tandem steps containing many intermediates.





The complicated mechanisms and product distribution make it extremely challenging to determine the reaction pathway. Many different pathways have been proposed. It is difficult to study the reaction kinetics before the reaction pathway is thoroughly investigated. The pressures of the reactants in Equation (6) are obtained by ignoring the influence of all the intermediates, while the value of I^α has not been well illustrated.

Here, the aim is to discuss the effects of light intensity and reaction temperature on the reaction rate law:

$$-r'_{CO_2} = f(T, I) \frac{P_{H_2O}P_{CO_2}}{(1 + K_{H_2O}P_{H_2O} + K_{CO_2}P_{CO_2})^2} \quad (15)$$

From Equations (11)–(14), it can be seen that light absorption and charge generation are analogous to a dissociation adsorption process. The saturated electron concentration can be analogously obtained as:

$$C_{e^-} = C_{h^+} = \frac{(KI)^{1/2}C_t}{1 + 2(KI)^{1/2}} \quad (16)$$

and the general rate law is then modified to:

$$-r'_{CO_2} = \frac{kI}{(1 + 2\sqrt{KI})^2} \frac{P_{H_2O}P_{CO_2}}{(1 + K_{H_2O}P_{H_2O} + K_{CO_2}P_{CO_2})^2}, \text{ with } k = k_iKC_t \quad (17)$$

where K is the ratio of the charge generation rate consistent with the charge recombination rate.

At the same time, as the global efficiency of CO_2 photoreduction is kept moderate, P_{H_2O} and P_{CO_2} may be assumed to be nearly equal to the initial concentration. The equation can be simplified to:

$$-r'_{CO_2} = \frac{kKC_tI}{(1 + 2\sqrt{KI})^2} c_0, \quad c_0 = \frac{P_{H_2O,0}P_{CO_2,0}}{(1 + K_{H_2O}P_{H_2O,0} + K_{CO_2}P_{CO_2,0})^2} \quad (18)$$

where $I = C_R I_0$, C_R is the light concentration ratio and I_0 is the original light intensity.

According to the relative reaction rate law, the following equation applies:

$$\frac{-r'_{CO_2}}{-1} = \frac{r_{HCs}}{1} \quad (19)$$

If the values of reaction temperature, light intensity, and hydrocarbons yield rate are measured and calculated, the reaction rate can be determined.

3.3. Reactor Model Development

The energy from the incident solar light has an impact on the reaction temperature of the CO_2 photoreduction reactor. Due to the irradiation intensity distribution, the temperature may be not homogeneous in the reactor and on the catalyst, which may influence the experimental results. An average value can thus be used to simply describe the influence of temperature and light intensity on the reaction, but to be more accurate, the distribution profile of these two parameters cannot be ignored.

A three-dimensional model of irradiation distribution on the catalyst surface and in the reactor was then established in the Tracepro software (TracePro Software, Littleton, USA, 2016), as shown in Figure 2. The scattering characteristic was modeled using the BRDF method in the Abg scattering function. The Monte-Carlo ray tracing method was applied for radiation propagation. Based on the irradiation distribution, the temperature

distribution on the catalyst surface was modeled using ANSYS-FLUENT 17.0 software (Canonsburg, PA, USA, 2016) [57].

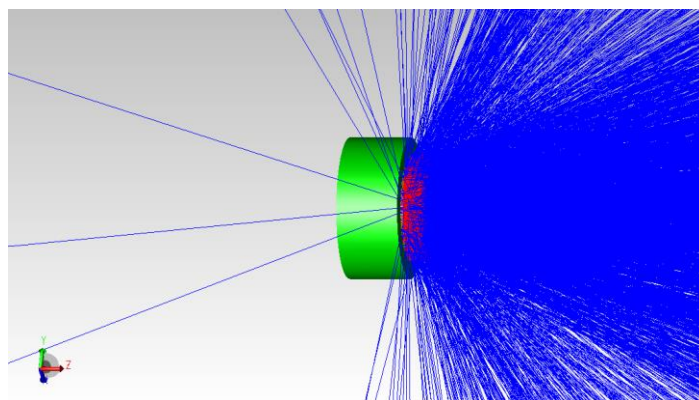


Figure 2. Irradiation distribution model on the catalyst surface and in the reactor.

To reduce the computational resource, the model was simplified according to the following assumptions:

1. The CO₂ photoreduction mainly happened on the top surface of the catalyst. The physical model was simplified to be two-dimensional.
2. Based on the round shapes of both the light source and catalyst, the physical model was considered to be axisymmetric.
3. According to the experimental results, the reaction rate and the conversion were relatively low, so the reaction heat was neglected.
4. The thickness of TiO₂ was 1 mm and the heat adsorption coefficient of TiO₂ was assumed to be 0.67.
5. The adsorption of incident radiation by the quartz glass window was neglected.
6. The flow of reactants was considered to be laminar, as the Reynolds number was $Re = 1.788 \times 0.2 \times 0.05 \div 0.0000137 = 1305.1$
7. The surface of the catalyst and the inner surface (side wall and bottom) of the reactor were considered as the internal heat source to join the boundary conditions. The heat adsorption coefficient of the steel reactor was assumed to be 0.85.
8. The reactor was an ideal batch reactor. The unsteady model was chosen in FLUENT. The mixture model was used for the multiphase reactants flow. Since the evaporation of H₂O occurred, the evaporation-condensation model was used. The diameter of the bubble was set to 0.0001 m. Considering the high temperature from the concentrating light, the semi-transparent medium (quartz glass), CO₂, and H₂O all participated in the radiative heat transfer, and the DO model was used for radiative heat transfer calculation. The boundary between the fluid and solid was set as the coupling boundary. By adding the internal heat source to the UDF, the solar absorption radiation was added to the first grid layer as the boundary condition. The side wall and bottom surface of the reactor were included in the boundary condition in the same way.
9. Convection and radiation heat transfer to the external environment was considered. The convective heat transfer coefficient with the outside air was calculated via the following expression:

$$0 \leq x \leq H, r = D/2 + l_{in} + l_{out} + l_s; -k_{out} \frac{\partial T}{\partial r} \Big|_+ = h(T_{out} - T_{\infty}), \quad (20)$$

$$Nu = \frac{hH}{k} = 0.664Re_D^{0.5}Pr^{0.5}, Re_D = \frac{v_{air}D}{\nu_{air}}$$

where v_{air} and ν_{air} are the velocity and viscosity of ambient air, respectively. According to the city environment, the wind speed is assumed to be 2 m/s, and the convective heat

transfer coefficient of the external wall to the outside air is $22 \text{ W}\cdot\text{m}^{-1}\cdot\text{K}^{-1}$. The grid size is 0.0008 m, and the grid independence was verified.

3.4. Catalytic Tests in the Concentrating Solar Light Reactor System

A TiO_2 (Degussa, Essen, Germany) catalyst was chosen to investigate the effect of the reactor system. It was calcined, compressed, and transformed into a disc shape with different sizes and settled into the reactor. Before reaction, the reactor was purged using nitrogen gas (99.999%, Jingong Co. Ltd., Hangzhou, China). Then, the reactant CO_2 gas (99.999%, Jingong Co. Ltd., Hangzhou) was injected. The initial pressure of the reactor was 0.1 MPa. The amount of water was 5.0 mL. The temperatures and pressures were recorded using a thermocouple and a pressure gauge. The products were collected and analyzed via a gas chromatograph (GC-2014, Shimadzu, Tokyo, Japan).

4. Results and Discussion

4.1. Modeling Results of Temperature Distribution in the Reactor

Figures 3 and 4 show the 2D irradiation distribution under simulated concentrating solar light. Based on the model results, the light is concentrated in the reactor and on the catalyst surface. The irradiation intensity follows a Gaussian distribution, and the temperature thus follows a similar distribution. The maximum temperature on the catalyst surface is about 430 K at a concentration of 16.

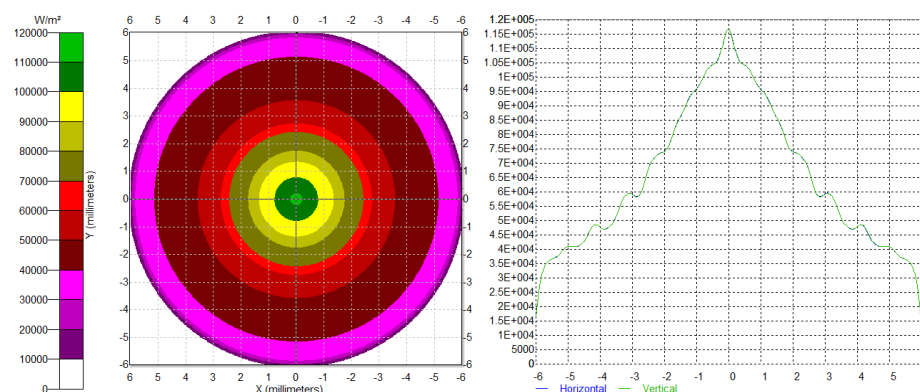


Figure 3. Modeled irradiation distribution on the catalyst surface: (left) schematic, (right) numeric.

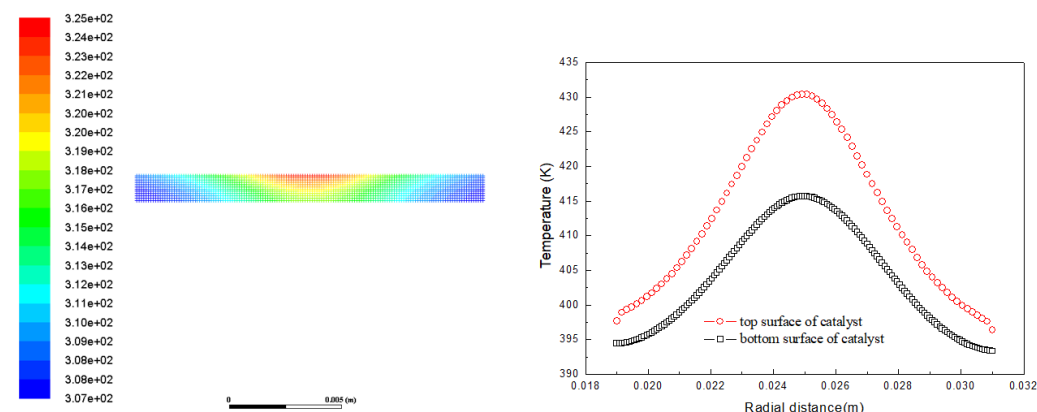


Figure 4. Modeled temperature distribution on the catalyst surface: (left) schematic, (right) numeric.

4.2. Experimental Temperature and Pressure Variation under Different Concentrating Ratios

The influence of the concentrating ratio on the temperature and pressure in the reactor was recorded under real solar light. Figure 5 displays the temperature variation of the catalyst disc on the horizontal axis under concentration ratios of 300, 400, 600, 800, and 1000. In general, the measured values of the temperature are in line with the modeling

results. The temperature reached a maximum at the center of the catalyst disc and gradually decreased to the edge and the reactants. With an increase in the concentrating ratio, the maximum temperature also increased. At a concentration ratio of 1000, the maximum temperature reached about 553 °C. As the temperature became higher than the crystal transformation temperature of Anatase TiO₂, the concentration ratio was not increased any more. Figure 6 displays the maximum pressure in the reactor. It can reasonably be considered that the maximum pressure increased with the concentrating ratio, as the reactants were heated to a higher temperature. When the concentrating ratio reached a value of 1000, the incident solar energy was concentrated in the center of the reactor and was entirely absorbed. The pressure would not increase further.

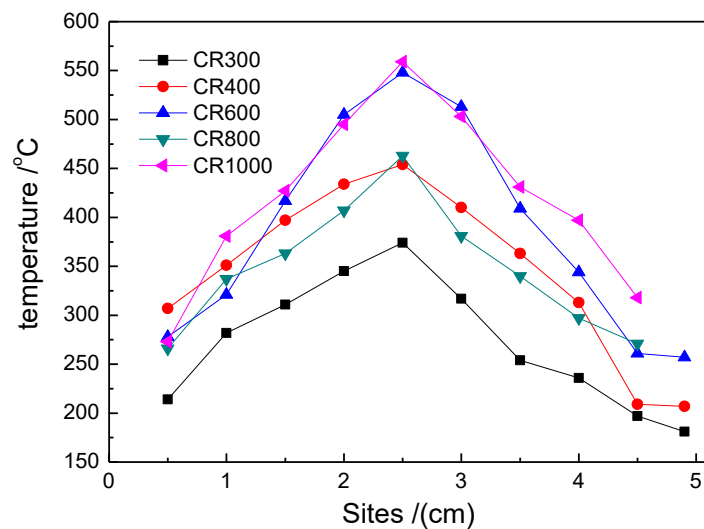


Figure 5. Temperature variation of the catalyst disc surface under different concentrating ratios. Conditions: 0.1 MPa CO₂, 0.5 mL H₂O, room temperature at about 20 °C, measured at noon.

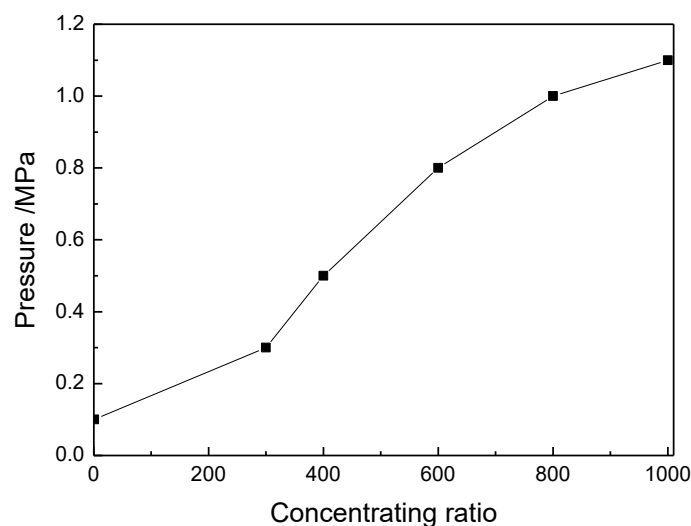


Figure 6. Maximum pressure in the reactor under different concentrating ratios.

4.3. Temperature and Pressure Variation under Different H₂O Contents

The reactants were considered to have an influence on the temperature and pressure in the reactor. Especially for H₂O, vaporization occurred when the temperature increased, which contributed to the pressure increase. Figure 7 displays the temperature variation of the catalyst disc on the horizontal axis under water contents of 0.5 mL and 0.8 mL. It can be seen that the temperature is clearly decreased (the maximum temperature decreases to below 300 °C).

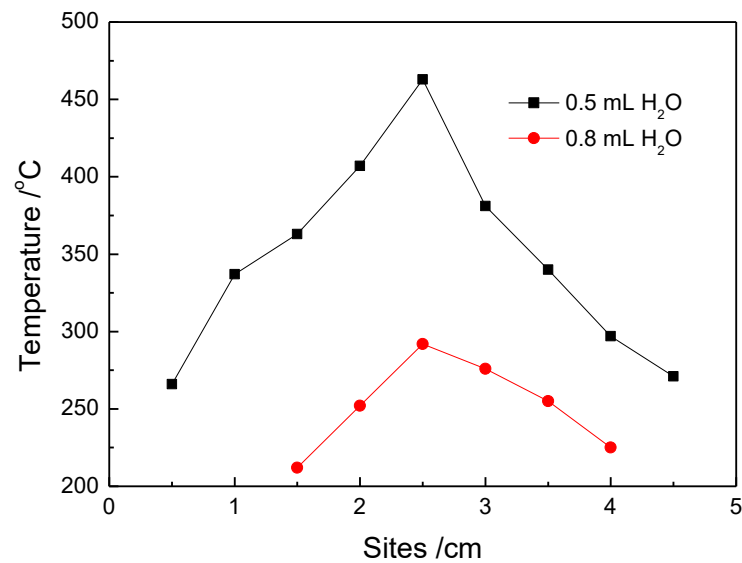


Figure 7. Temperature variation of the catalyst disc surface under different H₂O contents. Conditions: 0.1 MPa CO₂, concentrating ratio of 800, measured at noon.

4.4. Temperature and Pressure Variation under Different Room Temperatures

The temperature in the reactor is influenced by many factors. One unexpected factor is the environment temperature. Figure 8 displays the temperature variation of the catalyst disc on the horizontal axis under room temperatures of about 20, 30, and 40 °C. The temperature distribution is similar. However, when increasing the room temperature, the temperatures in the reactor are clearly increased. At a room temperature of 38 °C, the maximum temperature reaches near 800 °C. This means that the heat transfer of the reactor has to be improved in the future.

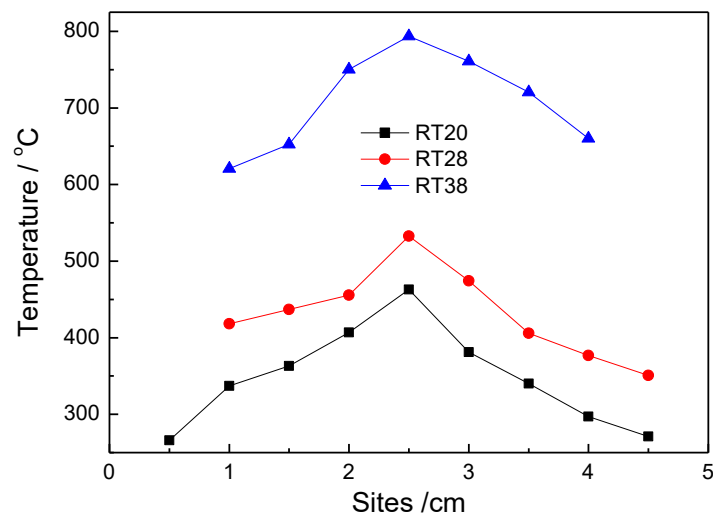


Figure 8. Temperature variation of the catalyst disc surface under different room temperatures. Conditions: 0.1 MPa CO₂, 0.5 mL H₂O, concentrating ratio of 800, measured at noon.

4.5. CO₂ Photoreduction Performance under Concentrated Solar Light

The concept of process intensification via the concentrated solar reaction system was then verified under simulated and real solar light, as shown in Figures 9 and 10.

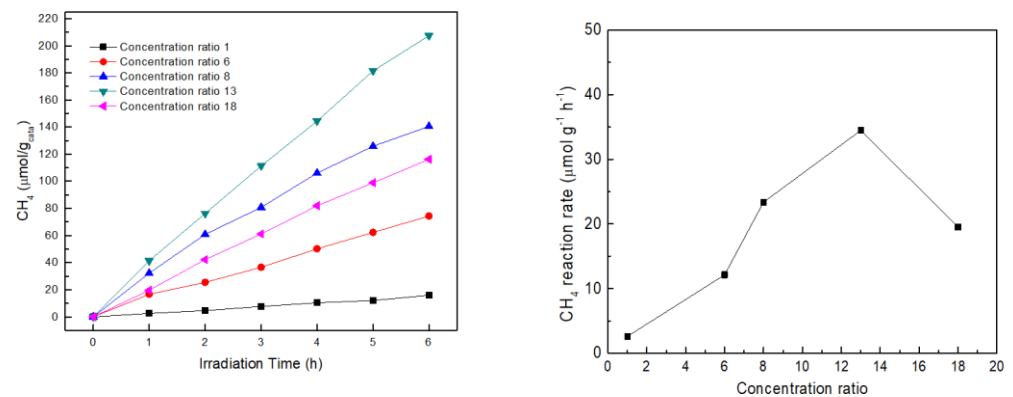


Figure 9. CH₄ yields and rate under simulated concentrating lights: (left) yield, (right) reaction rate.

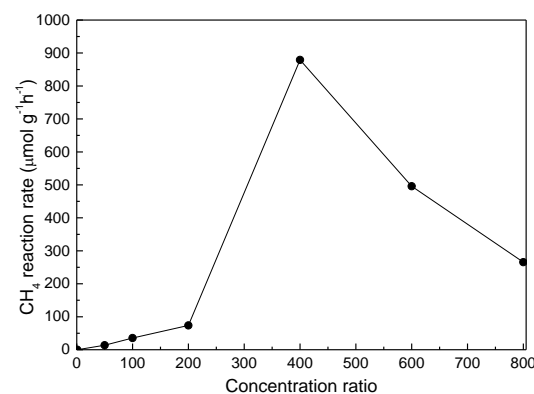


Figure 10. Reaction rate of CO₂ photoreduction under concentrating solar light. Hangzhou, AM10:30–PM2:30. The average solar light intensity is about 60 mW/cm².

According to the results, the concentrating technology can increase the CO₂ photoreduction rate for the considered concentrating ratios. The effects are more pronounced with a real solar light source under high concentrating ratios. The intensification of reaction conditions not only increased the reaction rate, but also enriched the evolved product species. Besides CH₄, both C₂H₄ and C₂H₆ were detected by the gas chromatograph (GC) (Figure 11). Considering the existence of C₂ species, the CO₂ photoreduction reaction efficiency was enhanced. The average reaction rate of CO₂ reduction reached 73.71, 879.14, 496, and 265.43 μmol·g⁻¹·h⁻¹ under the concentrating ratios of 200, 400, 600, and 800, respectively. Compared to the results without concentrating sunlight (about 0.1 μmol·g⁻¹·h⁻¹), the reaction rate can be increased by hundreds of times. In addition, the reaction rate curve showed a volcano type trend with the concentrating ratio increment, i.e., the reaction rate first increased with the concentrating ratio and then decreased. These results indicate that the factors controlling the global effect of concentrating ratio are complex. Considering the distribution of the light intensity on the catalyst surface and the associated temperature distribution, the reaction rate equation can be changed to:

$$-r'_{\text{CO}_2} = \sum \frac{k(T_j)I_jP}{(1 + 2\sqrt{KI_j})^2} \frac{P_{\text{H}_2\text{O}}P_{\text{CO}_2}}{(1 + K_{\text{H}_2\text{O}}P_{\text{H}_2\text{O}} + K_{\text{CO}_2}P_{\text{CO}_2})^2} \quad (21)$$

where P is the percentage of certain area with certain light intensity and temperature. It can be roughly averaged to the following equation, and further to Equations (18) and (19), where M represents the mean value.

$$-r'_{\text{CO}_2} = \frac{k(T_M)I_M}{(1 + 2\sqrt{KI_M})^2} \frac{P_{\text{H}_2\text{O}}P_{\text{CO}_2}}{(1 + K_{\text{H}_2\text{O}}P_{\text{H}_2\text{O}} + K_{\text{CO}_2}P_{\text{CO}_2})^2} \quad (22)$$

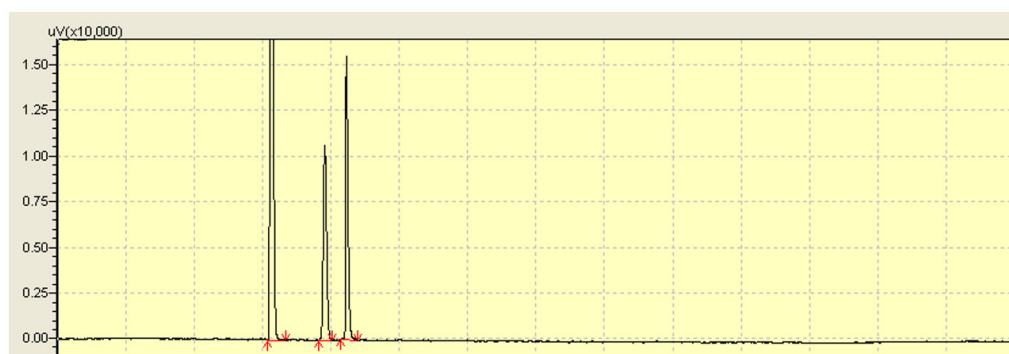


Figure 11. Original GC-map of CO₂ reduction products distribution. Conditions: 0.1 MPa CO₂, 0.5 mL H₂O, concentrating ratio of 800.

As the change in reaction conditions is slight under the simulated light source, the influence of temperature and light intensity distribution is relatively small. A reaction kinetics regression is performed using the experimental reaction rate data. The results are plotted in Figure 12. It can be seen that the data shows good linearity, and the slope, α , is just equal to 1. In this range, the reaction order of light intensity is 1. The controlling factor of the reaction rate is the light intensity.

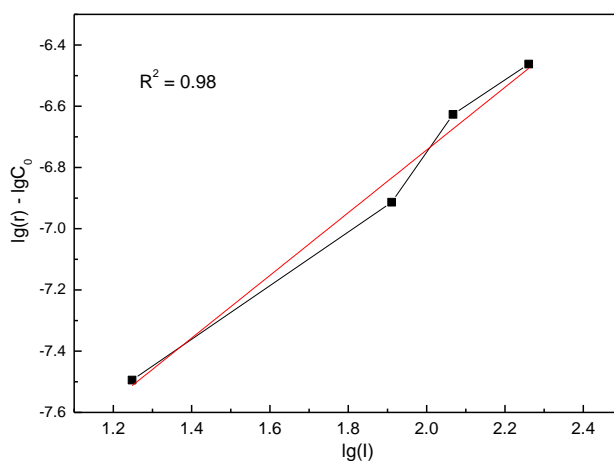


Figure 12. Regression of reaction kinetics data under simulated concentrating light.

5. Summary

In general, the recent reports about improvement of CO₂ photoreduction via process intensification have been reviewed in this work. The rising of light intensity, temperature and pressure are clearly beneficial to the CO₂ photoreduction rate. As a result, the concentrating solar technology, which can increase the light intensity, temperature, and pressure simultaneously, could be a relevant method to enhance the CO₂ photoreduction. The concept and experimental tests of CO₂ photoreduction under concentrating solar light are illustrated. A reactor design and a kinetic model were developed and discussed, and the different reaction parameters in the reactor were recorded. The intensification of reaction conditions via concentrating solar light technology can increase the reaction rate of CO₂ photoreduction by hundreds and even thousands of times. However, concentrating solar light technology also induces a distribution of the light intensity and temperature. More experimental devices and experiments need to be designed and carried out to get deeper understanding and faster progress of CO₂ photoreduction.

Author Contributions: Conceptualization, Z.Z.; methodology, Z.Z., Y.W.; investigation, Z.Z., H.L. (Huayan Liu); writing—original draft preparation, Z.Z.; writing—review and editing, Z.Z., Y.W., G.C.,

H.L. (Huayan Liu), S.A. and H.L. (Hanfeng Lu) All authors have read and agreed to the published version of the manuscript.

Funding: This work was supported by the Natural Science Foundation of China (No. 21506194, 21676255).

Data Availability Statement: The data presented in this study are available on request from the authors.

Acknowledgments: We thanks the help of Chang Zheshao about the discussion of model building.

Conflicts of Interest: The authors declare no conflict of interest.

References

1. Fu, Z.Y.; Yang, Q.; Liu, Z.; Chen, F.; Yao, F.B.; Xie, T.; Zhong, Y.; Wang, D.B.; Li, J.; Li, X.M.; et al. Photocatalytic conversion of carbon dioxide: From products to design the catalysts. *J. CO₂ Util.* **2019**, *34*, 63–73. [[CrossRef](#)]
2. Fujishima, A.; Honda, K. Electrochemical photolysis of water at a semiconductor electrode. *Nature* **1972**, *238*, 37–38. [[CrossRef](#)]
3. Tooru, I.; Akira, F.; Satoshi, K.; Honda, A. Photoelectrocatalytic reduction of carbon dioxide in aqueous suspensions of semiconductor powders. *Nature* **1979**, *277*, 637–638.
4. Shih, C.F.; Zhang, T.; Li, J.H.; Bai, C.L. Powering the future with liquid sunshine. *Joule* **2018**, *2*, 1–25. [[CrossRef](#)]
5. Gust, D.; Moore, T.A.; Moore, A.L. Solar Fuels via Artificial Photosynthesis. *Acc. Chem. Res.* **2009**, *42*, 1890–1898. [[CrossRef](#)]
6. Li, X.P.; Wang, L.; Su, W.; Xing, Y. A review of the research status of CO₂ photocatalytic conversion technology based on bibliometrics. *New J. Chem.* **2021**, *45*, 2315–2325. [[CrossRef](#)]
7. Moustakas, N.G.; Strunk, J. Photocatalytic CO₂ Reduction on TiO₂-Based Materials under Controlled Reaction Conditions: Systematic Insights from a Literature Study. *Chem. Eur. J.* **2018**, *24*, 12739–12746. [[CrossRef](#)] [[PubMed](#)]
8. Roy, S.C.; Varghese, O.K.; Paulose, M.; Grimes, C.A. Toward Solar Fuels: Photocatalytic Conversion of Carbon Dioxide to Hydrocarbons. *ACS Nano* **2010**, *4*, 1259–1278. [[CrossRef](#)] [[PubMed](#)]
9. Sorcar, S.; Yoriya, S.; Lee, H.; Grimes, C.A.; Feng, S.P. A review of recent progress in gas phase CO₂ reduction and suggestions on future advancement. *Mater. Today Chem.* **2020**, *16*, 100264. [[CrossRef](#)]
10. Hisatomi, T.; Domen, K. Introductory lecture: Sunlight-driven water splitting and carbon dioxide reduction by heterogeneous semiconductor systems as key processes in artificial photosynthesis. *Faraday Discuss.* **2016**, *198*, 11–35. [[CrossRef](#)] [[PubMed](#)]
11. Teramura, K.; Tanaka, T. Necessary and sufficient conditions for the successful three-phase photocatalytic reduction of CO₂ by H₂O over heterogeneous photocatalysts. *Phys. Chem. Chem. Phys.* **2018**, *20*, 8423–84316. [[CrossRef](#)]
12. Chang, X.X.; Wang, T.; Gong, J.L. CO₂ photo-reduction: Insights into CO₂ activation and reaction on surfaces of photocatalysts. *Energy Environ. Sci.* **2016**, *9*, 2177–2196. [[CrossRef](#)]
13. Kondratenko, E.V.; Mul, G.; Baltrusaitis, J.; Larrazbál, G.O.; Pérez-Ramírez, J. Status and perspectives of CO₂ conversion into fuels and chemicals by catalytic, photocatalytic and electrocatalytic processes. *Energy Environ. Sci.* **2013**, *6*, 3112–3137. [[CrossRef](#)]
14. He, J.; Janáky, C. Recent Advances in Solar-Driven Carbon Dioxide Conversion: Expectations versus Reality. *ACS Energy Lett.* **2020**, *5*, 1996–2014. [[CrossRef](#)]
15. Fang, Y.X.; Wang, X.C. Photocatalytic CO₂ conversion by polymeric carbon nitrides. *Chem. Commun.* **2018**, *54*, 5674–5687. [[CrossRef](#)]
16. Habisreutinger, S.N.; Schmidtmeide, L.; Stolarczyk, J.K. Photocatalytic reduction of CO₂ on TiO₂ and other semiconductors. *Angew. Chem. Int. Ed.* **2013**, *52*, 7372–7408. [[CrossRef](#)] [[PubMed](#)]
17. Jiao, X.C.; Zheng, K.; Liang, L.; Li, X.D.; Sun, Y.F.; Xie, Y. Fundamentals and challenges of ultrathin 2D photocatalysts in boosting CO₂ photoreduction. *Chem. Soc. Rev.* **2020**, *49*, 6592–6604. [[CrossRef](#)] [[PubMed](#)]
18. Zhang, W.H.; Mohamed, A.R.; Ong, W.J. Z-Scheme Photocatalytic Systems for Carbon Dioxide Reduction: Where Are We Now? *Angew. Chem. Int. Ed.* **2020**, *59*, 22894–22915. [[CrossRef](#)]
19. Izumi, Y. *Recent Advances (2012–2015) in the Photocatalytic Conversion of Carbon Dioxide to Fuels Using Solar Energy: Feasibility for a New Energy*; Advances in CO₂ Capture, Sequestration, and Conversion, ACS Symposium Series; American Chemical Society: Washington, DC, USA, 2015.
20. Nguyen, V.H.; Wu, J.C. Recent developments in the design of photoreactors for solar energy conversion from water splitting and CO₂ reduction. *Appl. Catal. A* **2018**, *550*, 122–141. [[CrossRef](#)]
21. Ulmer, U.; Dingle, T.; Duchesne, P.N.; Morris, R.H.; Tavasoli, A.; Wood, T.; Ozin, G.A. Fundamentals and applications of photocatalytic CO₂ methanation. *Nat. Commun.* **2019**, *10*, 3169–3181. [[CrossRef](#)]
22. Ghossou, M.; Xia, M.; Duchesne, P.N.; Segal, D.; Ozin, G. Principles of photothermal gas-phase heterogeneous CO₂ catalysis. *Energy Environ. Sci.* **2019**, *12*, 1122–1144. [[CrossRef](#)]
23. Khan, A.A.; Tahir, M. Recent advancements in engineering approach towards design of photoreactors for selective photocatalytic CO₂ reduction to renewable fuels. *J. CO₂ Util.* **2019**, *29*, 205–239. [[CrossRef](#)]
24. Kovacic, Ž.; Likozar, B.; Hus, M. Photocatalytic CO₂ Reduction: A Review of Ab Initio Mechanism, Kinetics, and Multiscale Modeling Simulations. *ACS Catal.* **2020**, *10*, 14984–15007. [[CrossRef](#)]

25. Mateo, D.; Cerrillo, J.L.; Durini, S.; Gascon, J. Fundamentals and applications of photo-thermal catalysis. *Chem. Soc. Rev.* **2021**, *50*, 2173–2210. [[CrossRef](#)]
26. Terlouw, T.; Bauer, C.; Rosa, L.; Mazzotti, M. Life cycle assessment of carbon dioxide removal technologies: A critical review. *Energy Environ. Sci.* **2021**, *14*, 1701–1721. [[CrossRef](#)]
27. Rej, S.; Bisetto, M.; Naldoni, A.; Fornasiero, P. Well-defined Cu₂O photocatalysts for solar fuels and chemicals. *J. Mater. Chem. A* **2021**, *9*, 5915–5951. [[CrossRef](#)]
28. Li, X.; Yu, J.G.; Jaroniec, M.; Chen, X.B. Cocatalysts for Selective Photoreduction of CO₂ into Solar Fuels. *Chem. Rev.* **2019**, *119*, 3962–4179. [[CrossRef](#)] [[PubMed](#)]
29. Nair, V.; Muçoz-Batista, M.J.; Fernández-Garca, M.; Luque, R.; Colmenares, J.C. Thermo-Photocatalysis: Environmental and Energy Applications. *ChemSusChem* **2019**, *12*, 2098–2116. [[CrossRef](#)] [[PubMed](#)]
30. Gerven, T.V.; Stankiewicz, A. Structure, Energy, Synergy, TimesThe Fundamentals of Process Intensification. *Ind. Eng. Chem. Res.* **2009**, *48*, 2465–2474. [[CrossRef](#)]
31. Tan, L.L.; Ong, W.J.; Chai, S.P.; Mohamed, A.R. Photocatalytic reduction of CO₂ with H₂O over graphene oxide supported oxygen-rich TiO₂ hybrid photocatalyst under visible light irradiation: Process and kinetic studies. *Chem. Eng. J.* **2017**, *308*, 248–255. [[CrossRef](#)]
32. Olivo, A.; Thompson, W.A.; Bayc, E.R.B.; Ghedini, E.; Menegazzo, F.; Maroto-Valer, M.; Signoretto, M. Investigation of process parameters assessment via design of experiments for CO₂ photoreduction in two photoreactors. *J. CO₂ Util.* **2020**, *36*, 25–32. [[CrossRef](#)]
33. Olivo, A.; Trevisan, V.; Ghedini, E.; Pinna, F.; Bianchi, C.L.; Naldoni, A.; Cruciani, G.; Signoretto, M. CO₂ photoreduction with water: Catalyst and process investigation. *J. CO₂ Util.* **2015**, *12*, 86–94. [[CrossRef](#)]
34. Khalilzadeh, A.; Shariati, A. Photoreduction of CO₂ over heterogeneous modified TiO₂ nanoparticles under visible light irradiation: Synthesis, process and kinetic study. *Sol. Energy* **2018**, *164*, 251–261. [[CrossRef](#)]
35. Delavari, S.; Amin, N.A.S. Photocatalytic conversion of CO₂ and CH₄ over immobilized titania nanoparticles coated on mesh: Optimization and kinetic study. *Appl. Energy* **2016**, *162*, 1171–1185. [[CrossRef](#)]
36. Singhal, N.; Kumara, U. Noble metal modified TiO₂: Selective photoreduction of CO₂ to hydrocarbons. *Mol. Catal.* **2017**, *439*, 91–99. [[CrossRef](#)]
37. Singh, V.; Beltran, I.J.C.; Ribot, J.C.; Nagpal, P. Photocatalysis deconstructed: Design of a new selective catalyst for artificial photosynthesis. *Nano Lett.* **2014**, *14*, 597–603. [[CrossRef](#)]
38. Wu, C.Z.; Xing, X.X.; Yang, G.; Tong, T.; Wang, M.; Bao, J.M. Understanding the generation of long-chain hydrocarbons from CO₂ and water using cobalt nanostructures and light. *J. Catal.* **2020**, *390*, 206–212. [[CrossRef](#)]
39. Song, C.Q.; Liu, X.; Xu, M.; Masi, D.; Wang, Y.; Deng, Y.C.; Zhang, M.T.; Qin, X.T.; Feng, K.; Yan, J.; et al. Photothermal Conversion of CO₂ with Tunable Selectivity Using FeBased Catalysts: From Oxide to Carbide. *ACS Catal.* **2020**, *10*, 10364–10374. [[CrossRef](#)]
40. Guo, J.L.; Duchesne, P.N.; Wang, L.; Song, R.; Xia, M.K.; Ulmer, U.; Sun, W.; Dong, Y.C.; Loh, J.Y.Y.; Kherani, N.P.; et al. High-Performance, Scalable, and Low-Cost Copper Hydroxyapatite for Photothermal CO₂ Reduction. *ACS Catal.* **2020**, *10*, 13668–13681. [[CrossRef](#)]
41. Bai, Y.; Yang, P.; Wang, P.; Xie, H.; Dang, H.; Ye, L. Semimetal bismuth mediated UV-vis-IR driven photo-thermocatalysis of Bi₄O₅I₂ for carbon dioxide to chemical energy. *J. CO₂ Util.* **2018**, *23*, 51–60. [[CrossRef](#)]
42. Zhang, L.; Kong, G.; Meng, Y.; Tian, J.; Zhang, L.; Wan, S.; Lin, J.; Wan, Y. Direct Coupling of Thermo- and Photocatalysis for Conversion of CO₂-H₂O into Fuels. *ChemSusChem* **2017**, *10*, 4709–4714. [[CrossRef](#)]
43. Li, Y.G.; Hao, J.C.; Song, H.; Zhang, F.Y.; Bai, X.H.; Meng, X.G.; Zhang, H.Y.; Wang, S.F.; Hu, Y.; Ye, J.H. Selective light absorber-assisted single nickel atom catalysts for ambient sunlight-driven CO₂ methanation. *Nat. Commun.* **2019**, *10*, 2359–2368. [[CrossRef](#)]
44. Li, R.Z.; Li, Y.; Li, Z.H.; Wei, W.Q.; Ouyang, S.X.; Yuan, H.; Zhang, T.R. A Metal-Segregation Approach to Generate CoMn Alloy for Enhanced Photothermal Conversion of Syngas to Light Olefins. *Sol. RRL* **2021**, *5*, 2000488. [[CrossRef](#)]
45. Matthews, R.W.; McEvoy, S.R. A comparison of 254 nm and 350 nm excitation of TiO₂ in simple photocatalytic reactors. *J. Photochem. Photobiol. A Chem.* **1992**, *66*, 355–366. [[CrossRef](#)]
46. Swearer, D.F.; Robotjazi, H.; Martirez, J.M.P.; Zhang, M.; Zhou, L.; Carter, E.A.; Nordlander, P.; Halas, N.J. Plasmonic Photocatalysis of Nitrous Oxide into N₂ and O₂ Using Aluminum-Iridium Antenna-Reactor Nanoparticles. *ACS Nano* **2019**, *13*, 8076–8086. [[CrossRef](#)] [[PubMed](#)]
47. Rej, S.; Mascaretti, L.; Santiago, E.Y.; Tomanec, O.; Kment, Š.; Wang, Z.; Zbořil, R.; Fornasiero, P.; Govorov, A.O.; Naldoni, A. Determining Plasmonic Hot Electrons and Photothermal Effects during H₂ Evolution with TiN-Pt Nanohybrids. *ACS Catal.* **2020**, *10*, 5261–5271. [[CrossRef](#)]
48. Rossetti, I.; Villa, A.; Pirola, C.; Prati, L.; Ramis, G. A novel high-pressure photoreactor for CO₂ photoconversion to fuels. *RSC Adv.* **2014**, *4*, 28883–28885. [[CrossRef](#)]
49. Bahadori, E.; Tripodi, A.; Villa, A.; Pirola, C.; Prati, L.; Ramis, G.; Dimitratos, N.; Wang, D.; Rossetti, I. High pressure CO₂ photoreduction using Au/TiO₂: Unravelling the effect of co-catalysts and of titania polymorphs. *Catal. Sci. Technol.* **2019**, *9*, 2253–2265. [[CrossRef](#)]
50. Guan, G.Q.; Kida, T.; Yoshida, A. Reduction of carbon dioxide with water under concentrated sunlight using photocatalyst combined with Fe-based catalyst. *Appl. Catal. B* **2003**, *41*, 387–396. [[CrossRef](#)]

51. Guan, G.Q.; Kida, T.; Harada, T.; Isayama, M.; Yoshida, A. Photoreduction of carbon dioxide with water over $K_2Ti_6O_{13}$ photocatalyst combined with Cu/ZnO catalyst under concentrated sunlight. *Appl. Catal. A* **2003**, *249*, 11–18. [[CrossRef](#)]
52. Nguyen, T.V.; Wu, J.C.S.; Chiou, C.H. Photoreduction of CO_2 over Ruthenium dye-sensitized TiO_2 -based catalysts under concentrated natural sunlight. *Catal. Commun.* **2008**, *9*, 2073–2076. [[CrossRef](#)]
53. Han, S.S.; Chen, Y.F.; Abanades, S.; Zhang, Z.K. Improving photoreduction of CO_2 with water to CH_4 in a novel concentrated solar reactor. *J. Energy Chem.* **2017**, *26*, 743–749. [[CrossRef](#)]
54. Li, D.; Chen, Y.F.; Abanades, S.; Zhang, Z.K. Enhanced activity of TiO_2 by concentrating light for photoreduction of CO_2 with H_2O to CH_4 . *Catal. Commun.* **2018**, *113*, 6–9. [[CrossRef](#)]
55. Fang, X.X.; Gao, Z.H.; Lu, H.F.; Zhang, Z.K. Boosting CO_2 photoreduction activity by large Fresnel lens concentrated solar light. *Catal. Commun.* **2019**, *125*, 48–51. [[CrossRef](#)]
56. Zhang, Z.K.; Gao, Z.H.; Liu, H.Y.; Abanades, S.; Lu, H.F. High Photothermally Active Fe_2O_3 Film for CO_2 Photoreduction with H_2O Driven by Solar Light. *ACS Appl. Energy Mater.* **2019**, *2*, 8376–8380. [[CrossRef](#)]
57. Chang, Z.S.; Li, X.; Xu, C.; Chang, C.; Wang, Z.F. Numerical simulation on the thermal performance of a solar molten salt cavity receiver. *Renew. Energy* **2014**, *69*, 324–335. [[CrossRef](#)]